Applied Catalysis B: Environmental 142–143 (2013) 780–784

Contents lists available at SciVerse ScienceDirect

Applied Catalysis B: Environmental

journal homepage: www.elsevier.com/locate/apcatb

On the origin of the optimum loading of Ag on Al_2O_3 in the C_3H_6-SCR of NO_x

Tesnim Chaieb[a,b], Laurent Delannoy[a,b], Catherine Louis[a,b], Cyril Thomas[a,b,*]

[a] UPMC, UMR 7197, Laboratoire de Réactivité de Surface, 4 Place Jussieu, F-75005 Paris, France
[b] CNRS, UMR 7197, Laboratoire de Réactivité de Surface, 4 Place Jussieu, F-75005 Paris, France

ARTICLE INFO

Article history:
Received 15 May 2013
Received in revised form 3 June 2013
Accepted 12 June 2013
Available online 24 June 2013

Keywords:
Ag/Al_2O_3
Selective Catalytic Reduction
Catalysts
NO_x-TPD
C_3H_6

ABSTRACT

Ag/Al_2O_3 catalysts synthesized by the common impregnation technique with various Ag loadings were characterized by the NO_x-Temperature-Programmed Desorption (TPD) method and their catalytic performances were evaluated in the selective catalytic reduction of NO_x by propene (C_3H_6-SCR). It was found that the NO_x uptake decreased linearly as the Ag surface density increased up to about 0.7 $Ag/nm^2_{Al_2O_3}$ and then leveled off. This behavior was attributed to the formation of a pseudo monolayer of Ag_2O clusters, i.e. to the maximum loading of silver per unit surface area of Al_2O_3 (0.7 $Ag/nm^2_{Al_2O_3}$) for which highly dispersed Ag_2O clusters are preserved on freshly calcined samples. It was also found that this optimum Ag surface density could be correlated to the catalytic performances in the C_3H_6-SCR of NO_x. The concept of Ag surface density allowed rationalizing some of the earlier results on C_3H_6-SCR of NO_x.

1. Introduction

To prevent global warming, which is partly attributable to the emissions of CO_2 from transportation vehicles, improved efficiency of the engines has been targeted to lower fuel consumption and hence CO_2 emissions. Lean burn engines, used in gasoline and diesel powered vehicles and operating in an excess of O_2, are intrinsically more fuel-efficient than the gasoline engines developed earlier, which typically operated under stoichiometric conditions [1]. Yet oxygen-rich exhausts make the Three-Way Catalysts, usually containing bimetallic Pt–Rh or Pd–Rh systems, developed in the early 1980s ineffective in the reduction of the nitrogen oxides (NO and NO_2: NO_x) produced by lean burn engines [1].

Miyadera first reported on the promising potential of the Ag/Al_2O_3 system for the Selective Catalytic Reduction of NO_x by various hydrocarbons (HC-SCR) [2], due to its elevated selectivity in N_2 compared to the platinum group metals-supported catalysts as reported by Burch [1]. Moreover, Miyadera revealed the existence of an optimum loading of silver (2 wt%) on alumina in the C_3H_6-SCR reaction [2]. To date, the existence of such an optimum loading of Ag has been confirmed by several groups [3–8] for Ag/Al_2O_3 samples prepared via the commonly used impregnation technique. Other groups reported that Ag(2 wt%)/Al_2O_3 catalysts exhibited higher C_3H_6-SCR performances than Ag/Al_2O_3 samples containing much higher Ag loadings [9–11]. In contrast, few studies concluded to an optimum Ag loading either much lower [12] or much higher [13] than 2 wt%.

The reason for the existence of an optimum Ag loading for Ag/Al_2O_3 catalysts in the C_3H_6-SCR of NO_x has not been clearly understood to date. Studies have almost exclusively focused on the characterization of the Ag phases [3–11,13]. The characterization of the Ag phases is not trivial and it has been shown that various silver species are present on the Ag/Al_2O_3 materials [14 and references therein], such as Ag_2O clusters or Ag^+ ions, electron-deficient Ag clusters ($Ag_n^{\delta+}$), although the presence of $Ag_n^{\delta+}$ species under the HC-SCR reaction is still being debated [15], and metallic Ag^0 nanoparticles and clusters. Several groups have concluded that Ag is predominantly present as Ag_2O clusters over all range of Ag loadings [9,16]. For the highest Ag loadings, however, larger Ag_2O clusters can be reduced to Ag^0 nanoparticles in the course of the HC-SCR reaction [4,9,17]. This would account for the observed decrease in the C_3H_6-SCR performances of highly-loaded Ag/Al_2O_3 catalysts due to the preferential oxidation of the hydrocarbon reductant on the Ag^0 nanoparticles, at the expense of its use for the reduction of NO_x on the oxidized Ag species [2,9,17].

To date, the work reported by Wang et al. [18] is the only study in which the influence of the Ag loading was investigated from "the point of view of changes in the surface properties of the Al_2O_3

* Corresponding author at: UPMC, UMR 7197, Laboratoire de Réactivité de Surface, 4 Place Jussieu, Case 178, F-75005 Paris, France. Tel.: +33 1 44 27 36 30; fax: +33 1 44 27 60 33.
E-mail address: cyril.thomas@upmc.fr (C. Thomas).

0926-3373/$ – see front matter © 2013 Elsevier B.V. All rights reserved.
http://dx.doi.org/10.1016/j.apcatb.2013.06.010

support". Recently, we proposed that the surfaces of oxides, which is typically the case of the Ag/Al_2O_3 system, could be characterized by the adsorption of NO_x followed by their temperature-programmed desorption (NO_x-TPD [19,20]) and we reported that the introduction of Ag on Al_2O_3 led to a decrease in the amount of NO_x stored on Al_2O_3 [21], suggesting that the NO_x species would only be chemisorbed on the Al_2O_3 sites free of Ag. The aim of the present work is to gain further understanding on the origin of the existence of an optimum Ag loading in the Ag/Al_2O_3 samples prepared by impregnation for the C_3H_6-SCR of NO_x via the characterization of the available Al_2O_3 surface in Ag/Al_2O_3 catalysts by NO_x-TPD.

2. Experimental

2.1. Catalyst synthesis and characterization

The γ-Al_2O_3 support (Procatalyse, 180 m^2/g) was ground and sieved, and the fraction between 0.200 and 0.315 mm was used to prepare the Ag-promoted samples. The introduction of Ag was performed by incipient wetness impregnation of the bare Al_2O_3 support (0.7 cm^3/g porous volume) by aqueous solutions of $AgNO_3$ (Aldrich, >99%) to achieve silver loadings varying from 0.5 to 4.3 wt%, which were ascertained by inductively coupled plasma atomic emission spectroscopy (ICP-AES, CNRS – Solaize). After impregnation, the Ag-loaded samples were aged for 4 h under ambient conditions and subsequently dried at 100 °C overnight. Finally, the Ag-loaded samples were calcined at 600 °C (3 °C/min) for 4 h in a muffle furnace. From here on, the samples will be denoted as $Ag(x)/Al_2O_3$, where x represents the Ag surface density expressed as the number of Ag atoms per nm^2 of support ($Ag/nm^2_{Al_2O_3}$), in which the BET surface of the sample was corrected for the content of Ag as Ag_2O, although this correction is less critical than that which must be done for tungstated zirconias with high W loadings [20].

N_2-sorption measurements were carried out on a Belsorp max instrument (Bel Japan) at 77 K after evacuation of the samples at 300 °C for 3 h.

2.2. C_3H_6-SCR runs

The steady state catalytic experiments were carried out in a U-type quartz reactor (12 mm i.d.). It is important to note that in contrast with most of the studies published to date, the amount of silver introduced in the catalyst bed was maintained constant. The samples were held on plugs of quartz wool and consisted in 0.38 g of mechanical mixtures of $Ag(x)/Al_2O_3$ and Al_2O_3 of the same grain sizes in which the amount of Ag was equal to 30.9 ± 1.2 μmol. The temperature of the tubular furnace was set by a Eurotherm 2408 temperature controller using a K type thermocouple. Prior to the C_3H_6-SCR experiments, the samples were calcined in situ in O_2(20%)-He at 550 °C (3 °C/min) for 2 h with a flow rate of 100 mL_{NTP}/min. After cooling down to 150 °C, the samples were exposed to the C_3H_6-SCR reaction mixture. NO (4000 ppm/He), C_3H_6 (2000 ppm/He), O_2 (100%) and He (100%) were fed from independent mass flow controllers (Brooks 5850TR). Typically, the composition of the C_3H_6–NO–O_2–He reaction mixture was: 400 ppm C_3H_6, 385 ppm NO_x (~96% NO) and 8% O_2 in He, and the total flow rate was 230 mL_{NTP}/min. The temperature was increased stepwise from 150 to 550 °C with 25 °C increments and left for about 1 h at each temperature step. The reactor outflow was analyzed using a μ-GC (Varian, CP4900) equipped with two channels. The first channel, a 5A molecular sieve column (80 °C, 150 kPa He, 200 ms injection time, 30 s backflush time), was used to separate N_2, O_2 and CO. The second channel, equipped with a poraplot Q column (60 °C, 150 kPa He, 200 ms injection time), was used to separate CO_2, N_2O, C_3H_6 and H_2O. A chemiluminescence NO_x analyzer (Thermo Environmental Instruments 42C-HT) allowed the simultaneous detection of both NO and NO_2. NO_x conversions to N_2 were calculated as follows:

$$X\ NO_x\ to\ N_2(\%) = \frac{2 \times [N_2]}{[NO_x]_{inlet} \times 100} \quad (1)$$

where $[NO_x]_{inlet}$ and $[N_2]$ were the concentrations in NO_x and N_2 measured at the inlet and the outlet of the reactor, respectively. Minute amounts of N_2O, below 5 ppm, were also detected. C_3H_6 conversions were calculated on the basis of the CO_x ($CO + CO_2$) products formed:

$$X\ C_3H_6(\%) = \frac{[CO] + [CO_2]}{[C_3H_6]_{inlet} \times 3} \times 100 \quad (2)$$

where [CO], $[CO_2]$ and $[C_3H_6]_{inlet}$ were the concentrations of CO and CO_2 measured at the outlet of the reactor and that of C_3H_6 measured at the inlet of the reactor, respectively.

2.3. NO_x-TPD experiments

Prior to the NO_x-TPD experiments, the samples were calcined in situ in O_2(20%)–He at 500 °C (3 °C/min) for 2 h with a flow rate of 100 mL_{NTP}/min. The samples (about 0.2 g of $Ag(x)/Al_2O_3$) were firstly contacted with a NO–O_2–He (385 ppm–8% – balance, 230 mL_{NTP}/min) mixture at room temperature (RT) until recovery of the inlet NO_x concentration. The samples were then flushed with O_2(8%)–He at RT to remove weakly chemisorbed NO_x species until the disappearance of the NO_x species in the O_2–He stream. The NO_x-TPD experiments were carried out from RT to 600 °C, at a heating rate of 3 °C/min. The reactor outflow was continuously monitored using the abovementioned chemiluminescence NO_x detector.

Table 1
Compositions, surface areas and Ag densities of the studied samples.

$Ag(x)/Al_2O_3$*		Surface area		Ag surface density	
Catalysts	Ag (wt%)	m^2/g	$m^2/g_{Al_2O_3}$	$Ag/nm^2_{Al_2O_3}$**	mg Ag/m^2
Al_2O_3	0.00	180	180	0.00	0.00
$Ag(0.1)/Al_2O_3$	0.46	179	180	0.14	0.03
$Ag(0.3)/Al_2O_3$	0.88	176	178	0.28	0.05
$Ag(0.4)/Al_2O_3$	1.33	178	181	0.41	0.07
$Ag(0.6)/Al_2O_3$	1.81	175	183	0.57	0.10
$Ag(0.7)/Al_2O_3$	2.18	179	182	0.67	0.12
$Ag(0.8)/Al_2O_3$	2.59	177	182	0.79	0.15
$Ag(0.9)/Al_2O_3$	3.06	176	182	0.94	0.17
$Ag(1.1)/Al_2O_3$	3.46	176	182	1.06	0.20
$Ag(1.3)/Al_2O_3$	4.28	174	183	1.31	0.25

* Where x represents the Ag surface density in $Ag/nm^2_{Al_2O_3}$.

** Ag surface density corrected for the content of Ag as Ag_2O following the procedure described in ref. [20].

3. Results and discussion

Table 1 shows that the contents of Ag varied from 0 to 4.3 wt% in the $Ag(x)/Al_2O_3$ catalysts. The BET surface area of these samples was found to be close to that of the bare Al_2O_3 support and the surface area calculated per g of Al_2O_3, when corrected for the content of Ag as Ag_2O, remained essentially constant ($180 \pm 3\ m^2/g_{Al_2O_3}$). The Ag surface densities were found to vary from 0.0 to 1.3 $Ag/nm^2_{Al_2O_3}$.

The catalytic performances of the $Ag(x)/Al_2O_3$ samples in the C_3H_6-SCR of NO_x are shown in Fig. 1. As expected from earlier studies [2–8], the $Ag(0.6)/Al_2O_3$ and $Ag(0.7)/Al_2O_3$ catalysts, with Ag loadings close to 2 wt% (Table 1), showed optimum conversions of NO_x to N_2 (Fig. 1a). $Ag(0.4)/Al_2O_3$ also exhibited conversion as high as that of the aforementioned samples but at slightly

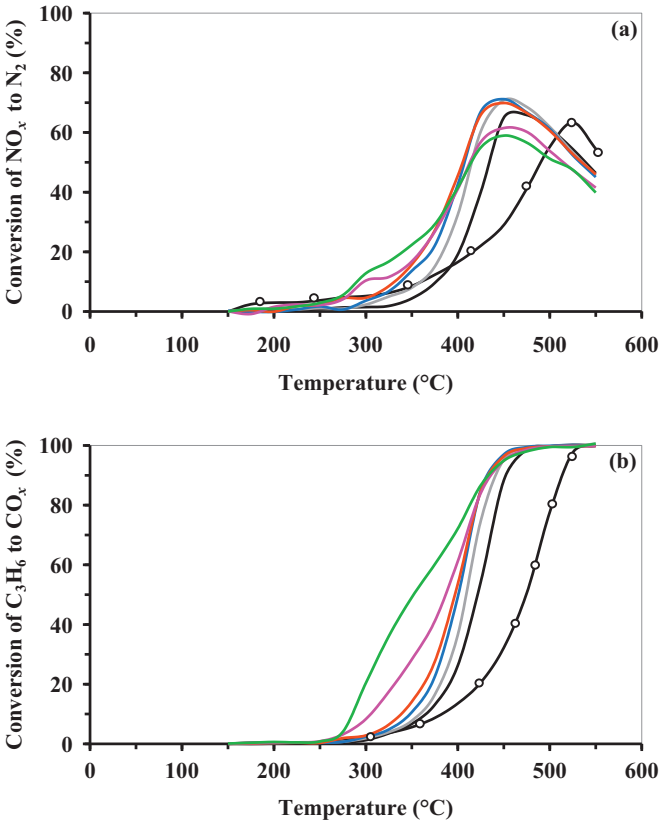

Fig. 1. (a) NO_x conversion to N_2 and (b) C_3H_6 conversion to CO_x vs. reaction temperature for Al_2O_3 (—O—), Ag(0.3)/Al_2O_3 (black), Ag(0.4)/Al_2O_3 (grey), Ag(0.6)/Al_2O_3 (blue), Ag(0.7)/Al_2O_3 (red), Ag(0.8)/Al_2O_3 (purple) and Ag(1.1)/Al_2O_3 (green). (For interpretation of the references to color in figure legend, the reader is referred to the web version of the article.)

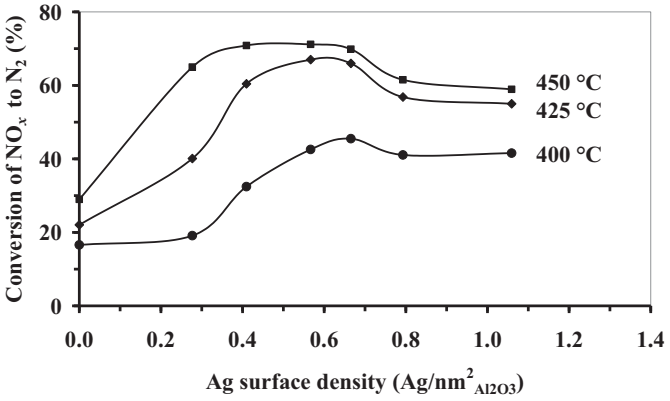

Fig. 2. NO_x conversion to N_2 at various reaction temperatures as a function of the Ag surface density.

higher temperatures, whereas the performances of Ag(0.3)/Al_2O_3 were clearly lower than those of the previous samples. This was also the case for the highly-loaded catalysts (Ag(0.8)/Al_2O_3 and Ag(1.1)/Al_2O_3) although it can also be seen that these samples showed slightly higher conversions of NO_x to N_2 than Ag(0.6)/Al_2O_3 and Ag(0.7)/Al_2O_3 below 375 °C (Fig. 1a). This particular behavior can be attributed to the better efficiency of the Ag(0.8)/Al_2O_3 and Ag(1.1)/Al_2O_3 catalysts to convert C_3H_6 at the lower temperatures (Fig. 1b), which results in a broadening of the NO_x reduction temperature window in line with earlier results [2]. Yet the higher activity of these two catalysts in propene oxidation also leads to a decrease in the NO_x conversion at high temperatures, the combustion of C_3H_6 occurring at the expense of its reaction with NO to produce N_2 [2]. The reason for the increased rate of C_3H_6 oxidation on the highly-loaded catalysts has been attributed to a decrease in the dispersion of Ag resulting from the formation of large Ag_2O clusters which could be reduced to Ag^0 particles by the hydrocarbons, the metallic Ag^0 particles being very active for the undesired complete oxidation of propene [4,9,17]. Fig. 2 summarizes the NO_x conversions to N_2 as a function of the Ag surface density at temperatures of 400, 425 and 450 °C. As mentioned above, a decrease in NO_x conversion is observed for Ag surface densities greater than 0.7 $Ag/nm^2_{Al_2O_3}$ at any temperature, hence for Ag loadings higher than 2.2 wt% (Table 1). Overall, below 0.7 $Ag/nm^2_{Al_2O_3}$, an increase in the C_3H_6-SCR performances is observed with an increase in Ag surface density, although the amount of Ag in the Ag(x)/Al_2O_3–Al_2O_3 mechanical mixture was kept constant (Section 2.2). It can also be noted from Fig. 2 that the range of Ag surface densities with optimum conversion of NO_x to N_2 broadens as the temperature increases, in agreement with earlier investigations [2].

For the sake of clarity, only the NO_x-TPD profiles of some of the Ag(x)/Al_2O_3 samples are shown in Fig. 3. These NO_x-TPD profiles exhibit low temperature (LT < 350 °C) and high temperature (HT > 350 °C) desorption peaks, in line with earlier investigations [21]. Such desorption profiles are consistent with those reported by Guo and co-workers obtained after exposure of Ag/Al_2O_3 samples to NO–O_2–He (1000 ppm – 8% -balance) at RT [22,23], thus under experimental conditions close to those reported in the present work. Fig. 3a shows that the addition of increasing contents of Ag leads to a decrease in the intensity of both peaks up to an Ag surface density of about 0.8 $Ag/nm^2_{Al_2O_3}$, which suggests that the NO_x species do not chemisorb on the Ag species, presumably Ag_2O clusters for freshly calcined samples [9,15,16]. A similar conclusion has been drawn by Sazama et al. [24] on the basis of FTIR measurements carried out on Al_2O_3 and an Ag/Al_2O_3 sample (1.76 wt% Ag), albeit at somewhat higher temperatures (~200 °C). In agreement with the conclusions of Sazama et al. [24], this indicates that Ag has blocked part of the Al_2O_3 sites available for NO_x chemisorption. For Ag surface densities higher than 0.8 $Ag/nm^2_{Al_2O_3}$ the intensity of the NO_x-TPD profiles remains essentially constant (Fig. 3a). The temperature at maximum NO_x desorption of the HT peak shifts slightly to lower temperatures ($\Delta T \sim 20$ °C) with increasing Ag surface density, whereas the temperature at maximum NO_x desorption of the LT peak shifts to higher temperatures ($\Delta T \sim 70$ °C) (Fig. 3a). The shift of the NO_x HT peak to slightly lower temperatures can be reasonably attributed to a decrease in the amounts of NO_x released. Such an explanation can not be accounted for the shift of the NO_x LT peak to higher temperatures, as in this particular case the amounts of NO_x released remain essentially constant for Ag surface densities greater than or equal to 0.8 $Ag/nm^2_{Al_2O_3}$ (Fig. 3). This shift of the NO_x LT peak to higher temperatures may be attributed to a strengthening in the bonding of the NO_x ad-species with increasing Ag loadings due to an increase in the basicity of Al_2O_3 with the introduction of increasing amounts of Ag [18].

In the case of tungstated zirconias, for which it was found that the NO_x species did not chemisorb on tungstates, we showed that the accessible surface of ZrO_2 was correlated with the NO_x uptake of the studied samples [19,20]. The NO_x uptakes of the Ag(x)/Al_2O_3 samples are summarized in Fig. 4. As in the case of the tungstated zirconias [19,20], the NO_x uptake decreases linearly with a rather good correlation coefficient ($R^2 = 0.94$) and then levels off. Taking into account the maximum deviation of the NO_x uptakes from the linear plot up to 0.8 $Ag/nm^2_{Al_2O_3}$, it can be concluded that the leveling off of the NO_x uptakes occurs at Ag surface densities greater than or equal to 0.7 $Ag/nm^2_{Al_2O_3}$, hence for silver loadings close to

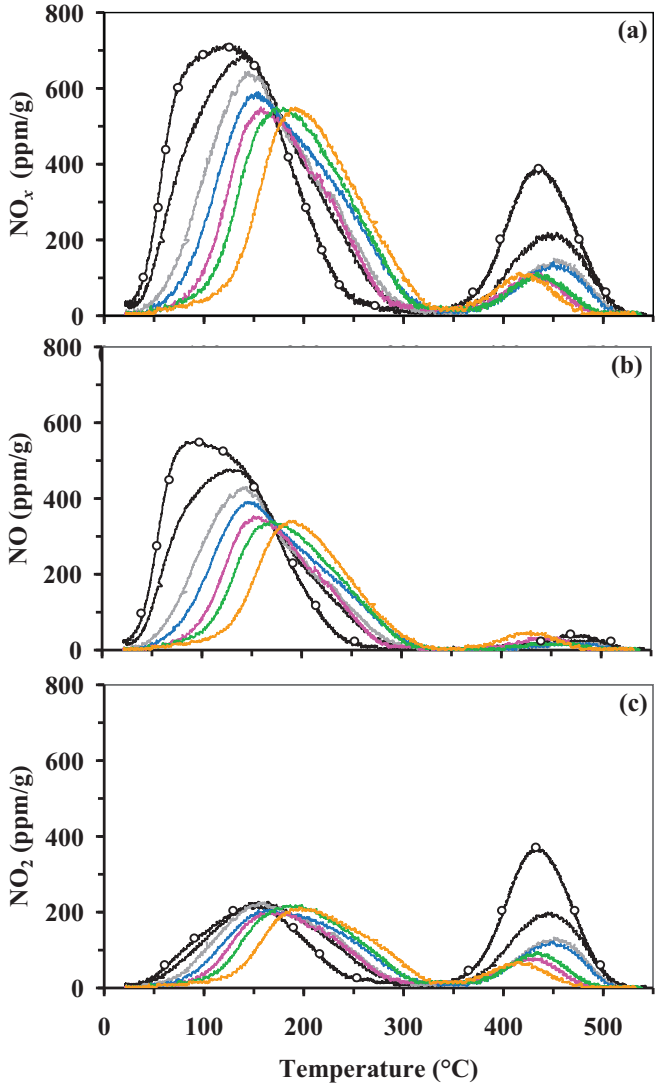

Fig. 3. (a) NO_x-, (b) NO- and (c) NO_2-TPD profiles of Al_2O_3 (—O—), Ag(0.3)/Al_2O_3 (black), Ag(0.4)/Al_2O_3 (grey), Ag(0.6)/Al_2O_3 (blue), Ag(0.8)/Al_2O_3 (purple), Ag(1.1)/Al_2O_3 (green) and Ag(1.3)/Al_2O_3 (orange). (For interpretation of the references to color in figure legend, the reader is referred to the web version of the article.)

2 wt% (Fig. 4). This suggests that pseudo monolayer coverage of Al_2O_3 by the Ag_2O clusters has been reached at such a Ag surface density/Ag loading. In other words, the Al_2O_3 surface sites onto which Ag is anchored are saturated for Ag surface densities greater than or equal to 0.7 Ag/$nm^2_{Al_2O_3}$ corresponding to Ag loadings close to 2 wt% (Fig. 4). At higher Ag surface densities/Ag loadings, this implies that the dispersion of Ag decreases. The slope of the line obtained in Fig. 4 ($-1.36\,\mu$mol $NO_x\,m^{-2}/Ag\,nm^{-2}_{Al_2O_3}$ = -0.8 NO_x molec./Ag atom), which indicates that 1 Ag atom prevents the adsorption of 0.8 molecule of NO_x, provides additional support for the existence of Ag in a highly dispersed state up to pseudo monolayer coverage, i.e. 0.7 Ag/$nm^2_{Al_2O_3}$ (2.2 wt% Ag). Breen et al. also concluded to the 0.7 Ag/$nm^2_{Al_2O_3}$ of Ag in a freshly calcined Ag(2 wt%)/Al_2O_3 sample by estimating an average Ag–Ag coordination number lower than unity by EXAFS [15].

It is remarkable that the Ag surface density for which maximum dispersion of Ag is achieved on Al_2O_3 (0.7 Ag/$nm^2_{Al_2O_3}$), as determined by the NO_x-TPD method (Fig. 4), also corresponds to the optimum composition for which maximum C_3H_6-SCR

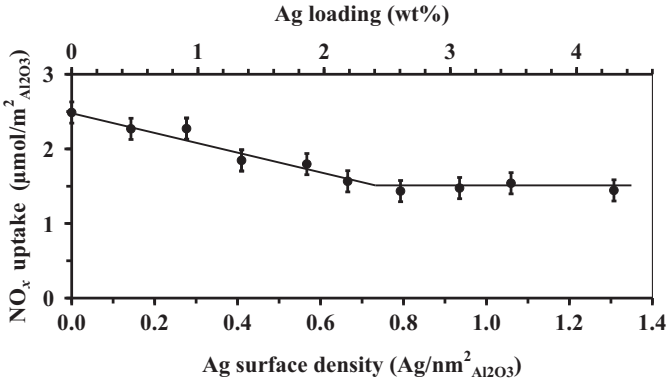

Fig. 4. NO_x uptakes as a function of the Ag surface density.

performances are observed in the present work (Figs. 1 and 2). Our catalytic results (Fig. 2) are also consistent with those reported previously in the literature for which a drop in the HC-SCR performances was observed for Ag surface densities greater than 0.7 Ag/$nm^2_{Al_2O_3}$ [2,4,5,8]. The use of this Ag surface density concept allows rationalizing some of the earlier results. As a first example, it can be found that the optimum Ag loading of Ag–Al_2O_3 catalysts in the C_3H_6-SCR reaction was 1.0 wt% in the studies reported by Meunier et al. [12]. In this work, however, the specific surface area of the bare Al_2O_3 support was lower (115 m^2/g, [12]) than those usually reported in comparable studies (152–260 m^2/g) [2,4,5,8]. Interestingly, Meunier et al. reported on an optimum composition of the Ag/Al_2O_3 catalysts in terms of Ag surface density, as they referred to an optimum silver loading of 0.087 mg/$m^2_{Al_2O_3}$ [12]. This optimum value, to which corresponds an Ag surface density of about 0.5 Ag/$nm^2_{Al_2O_3}$, is thus rather close to that reported in the present work and those that can be deduced from earlier studies [2,4,5,8]. In agreement with the results of the present study, Meunier et al. also found that the performances in the C_3H_6-SCR reaction of the Ag/Al_2O_3 catalysts decreased to a significant extent for Ag surface densities greater than or equal to 0.7 Ag/$nm^2_{Al_2O_3}$ (Ag loadings $\geq$1.5 wt%) [12]. As a second example, Jen [25] concluded that average pore size and pore-size distribution could be important factors for the catalytic performances of Ag(2 wt%)/Al_2O_3-*i* catalysts prepared with various starting Al_2O_3 supports (*i*). The author observed that the most active Ag samples (supported on Al_2O_3-1 and Al_2O_3-2 carriers) in the C_3H_6-SCR reaction were those exhibiting "the largest fractions of pores in the 15–100 Å range as well as the largest fractions in the most populated 50 Å range". Although there is no mention of the temperature at which the NO_x conversions were measured [25], the catalytic C_3H_6-SCR performances reported by Jen may also be rationalized in terms of Ag surface density of the studied Ag(2 wt%)/Al_2O_3-*i* samples. Indeed, we could calculate that their two most active catalysts, Ag/Al_2O_3-1 and Ag/Al_2O_3-2, displayed Ag surface densities of 0.5 and 0.6 Ag/$nm^2_{Al_2O_3}$, respectively, whereas the least active samples, Ag/Al_2O_3-3 and Ag/Al_2O_3-5, exhibited Ag surface densities of 0.4 and 1.2 Ag/$nm^2_{Al_2O_3}$, respectively. Considering the Ag surface density concept developed in the present study, the most active catalysts evaluated by Jen [25] displayed Ag surface densities (0.5 and 0.6 Ag/$nm^2_{Al_2O_3}$) similar to the optimum value (0.7 Ag/$nm^2_{Al_2O_3}$), as a plateau in the C_3H_6-SCR reaction dependence with the Ag surface density may exist depending on the temperature at which the catalytic performances are considered (Fig. 2). The lower C_3H_6-SCR performances of Ag/Al_2O_3-5 is explained by the fact that this sample exhibited a much higher Ag surface density (1.2 Ag/$nm^2_{Al_2O_3}$) than those of the optimum catalysts (0.6–0.7 Ag/$nm^2_{Al_2O_3}$, Figs. 2 and 4),

whereas those of Ag/Al_2O_3-3 can be related to its lower Ag surface density (0.4 $Ag/nm^2_{Al_2O_3}$), as also observed in our work (Fig. 2). Our concept does not apply, however, to the work of He et al. [13]. In this particular study, it was found that Ag/Al_2O_3 catalysts with much higher silver loadings than 2 wt % (4–8 wt%), – for Al_2O_3 supports of 210–240 m^2/g [13] and thus for Ag surface densities greater than 0.7 $Ag/nm^2_{Al_2O_3}$ and as high as 2.0 $Ag/nm^2_{Al_2O_3}$ – were much more active in the C_3H_6-SCR reaction than $Ag(2\ wt\%)/Al_2O_3$. To our knowledge, this study is the only one in which such a behavior has been reported. One can also note that the catalytic performances of the $Ag(2\ wt\%)/Al_2O_3$ reported by He et al. in the C_3H_6-SCR reaction [13] were found to be particularly low in the 200–500 °C range of temperatures.

Finally, the importance of the concept of Ag surface density has also been highlighted recently by Orlyk and co-workers in the C_2H_5OH-SCR of NO_x [26]. In their study, optimum catalytic performances were reported for surface concentrations of Ag of 0.09–0.13 mg/m^2. These values compare well with those reported by Meunier et al. (0.087 mg/m^2 [12]) and in the present work (0.07–0.12 mg/m^2, Table 1 and Fig. 1) in the case of the C_3H_6-SCR of NO_x.

4. Conclusion

Ag/Al_2O_3 catalysts with various Ag loadings were synthesized by the common impregnation technique and characterized by the NO_x-TPD method. It was found that the NO_x uptake decreased linearly with the Ag surface density up to about 0.7 $Ag/nm^2_{Al_2O_3}$ and then leveled off. This was attributed to the fact that the maximum dispersion of Ag_2O clusters is achieved at an optimum Ag surface density of about 0.7 $Ag/nm^2_{Al_2O_3}$, corresponding to an optimum Ag loading of about 2 wt%. It was also found that this optimum Ag surface density could be correlated to the catalytic performances in the C_3H_6-SCR of NO_x in terms of conversion of NO_x to N_2. For Ag surface densities higher than 0.7 $Ag/nm^2_{Al_2O_3}$, a decrease in the C_3H_6-SCR catalytic performances was observed, whereas at lower Ag surface densities the C_3H_6-SCR catalytic performances increased with increasing Ag surface densities. This work thus provides convincing arguments that the origin of the optimum Ag loading on Al_2O_3, reported to be about 2 wt% in the literature and deduced to be about 0.7 $Ag/nm^2_{Al_2O_3}$ according to the present study, results from the maximum loading of silver per unit surface area of Al_2O_3 for which Ag_2O clusters remain highly dispersed on freshly calcined samples. The use of the Ag surface density concept allowed rationalizing some of the earlier results on C_3H_6-SCR of NO_x.

Acknowledgment

T. Chaieb gratefully acknowledges UPMC for financial support (Grant 322/2012). Dr. Z.Y. Li (University of Birmingham) is acknowledged for critical reading of the manuscript.

References

[1] R. Burch, Catalysis Reviews Science and Engineering 46 (2004) 271.
[2] T. Miyadera, Applied Catalysis B: Environmental 2 (1993) 199.
[3] T.E. Hoost, R.J. Kulda, K.M. Collins, M.S. Chattha, Applied Catalysis B: Environmental 13 (1997) 59.
[4] K.-I. Shimizu, J. Shibata, H. Yoshida, A. Satsuma, T. Hattori, Applied Catalysis B: Environmental 30 (2001) 151.
[5] L.-E. Lindfors, K. Eränen, F. Klingstedt, D. Yu Murzin, Topics in Catalysis 28 (2004) 185.
[6] K. Arve, L. Čapek, F. Klingstedt, K. Eränen, L.-E. Lindfors, D.Y. Murzin, J. Dědeček, Z. Sobalik, B. Wichterlová, Topics in Catalysis 30/31 (2004) 91.
[7] R. Zhang, S. Kaliaguine, Applied Catalysis B: Environmental 78 (2008) 275.
[8] N.A. Sadokhina, A.F. Prokhorova, R.I. Kvon, I.S. Mashkovskii, G.O. Bragina, G.N. Baeva, V.I. Bukhtyarov, A. Yu Stakheev, Kinetics and Catalysis 53 (2013) 107.
[9] K.A. Bethke, H.H. Kung, Journal of Catalysis 172 (1997) 93.
[10] E. Seker, J. Cavataio, E. Gulari, P. Lorpongpaiboon, S. Osuwan, Applied Catalysis A: General 183 (1999) 121.
[11] H. Kannisto, H.H. Ingelsten, M. Skoglundh, Journal of Molecular Catalysis 302 (2009) 86.
[12] F.C. Meunier, R. Ukropec, C. Stapelton, J.R.H. Ross, Applied Catalysis B: Environmental 30 (2001) 163.
[13] H. He, C. Zhang, Y. Yu, Catalysis Today 90 (2004) 191.
[14] K.-I. Shimidzu, A. Satsuma, Physical Chemistry Chemical Physics 8 (2006) 2677.
[15] J.P. Breen, R. Burch, C. Hardacre, C.J. Hill, Journal of Physical Chemistry B 109 (2005) 4805.
[16] M. Richter, U. Bentrup, R. Eckelt, M. Schneider, M.-M. Pohl, R. Fricke, Applied Catalysis B: Environmental 51 (2004) 261.
[17] N. Bogdanchikova, F.C. Meunier, M. Avalos-Borja, J.P. Breen, A. Pestryakov, Applied Catalysis B: Environmental 36 (2002) 287.
[18] Z.-M. Wang, M. Yamaguchi, I. Goto, M. Kumagai, Physical Chemistry Chemical Physics 2 (2000) 3007.
[19] H.Y. Law, J. Blanchard, X. Carrier, C. Thomas, Journal of Physical Chemistry C 114 (2010) 9731.
[20] C. Thomas, Journal of Physical Chemistry C 115 (2011) 2253.
[21] J. Blanchard, R.P. Doherty, H.Y. Law, C. Méthivier, C. Thomas, Topics in Catalysis 56 (2013) 134.
[22] Y. Guo, M. Sakurai, H. Kameyama, Applied Catalysis B: Environmental 79 (2008) 382.
[23] Y. Guo, J. Chen, H. Kameyama, Applied Catalysis A: General 397 (2011) 163.
[24] P. Sazama, L. Čapek, H. Drobná, Z. Sobalík, J. Dědeček, K. Arve, B. Wichterlová, Journal of Catalysis 232 (2005) 302.
[25] H.-W. Jen, Catalysis Today 42 (1998) 37.
[26] N. Popovych, P. Kirienko, S. Soloviev, S. Orlyk, Catalysis Today 191 (2012) 38.